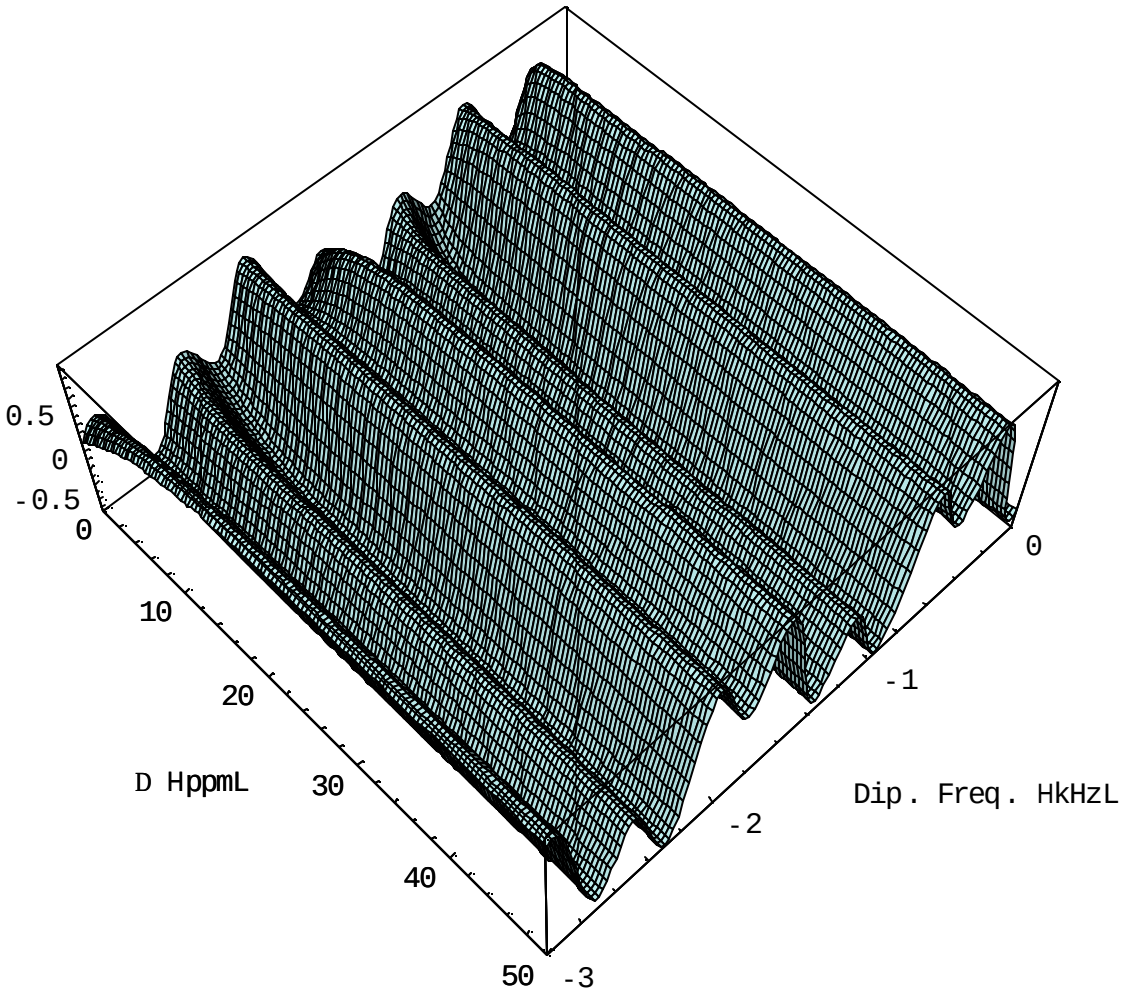

Figure 5-11: Graph of the CT function for the Ix self-magnetization, when $\sigma(0)=Ix$ for an oriented sample,, as a function of the dipolar coupling frequency in the lab frame in kHz, and the chemical shift difference Δ in the lab frame where t=3ms,and the CS average frequency in the lab frame is set as Σ =50 ppm. The scalar coupling J=0.

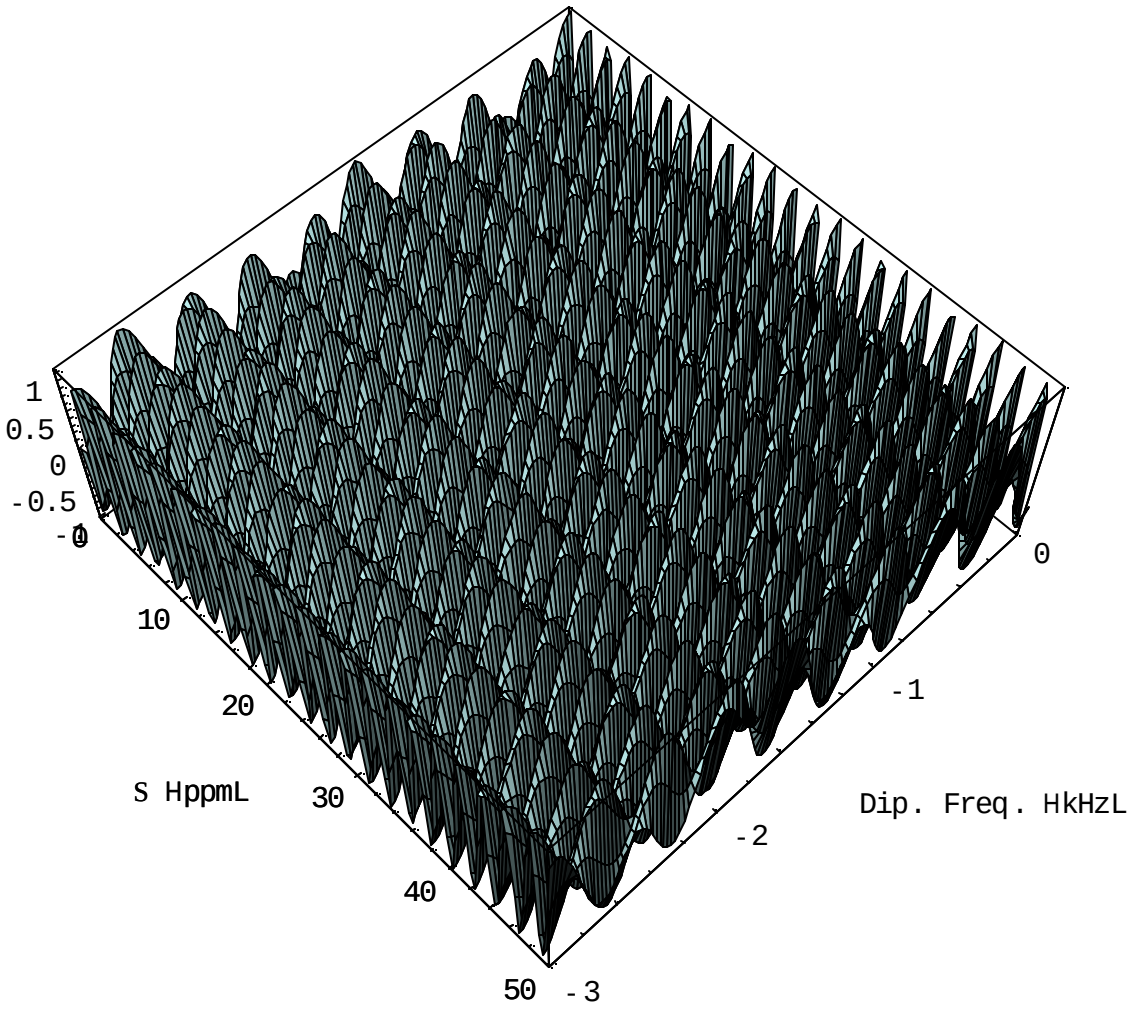

Figure 5-12: Graph of the CT function for the Ix self-magnetization for an oriented sample,, when $\sigma(0)=Ix$, as a function of the dipolar coupling frequency in the lab frame in kHz, and the chemical shift average Σ in the lab frame where t=3ms,and the CS average frequency in the lab frame is set as Δ=50ppm; The scalar coupling J=0.

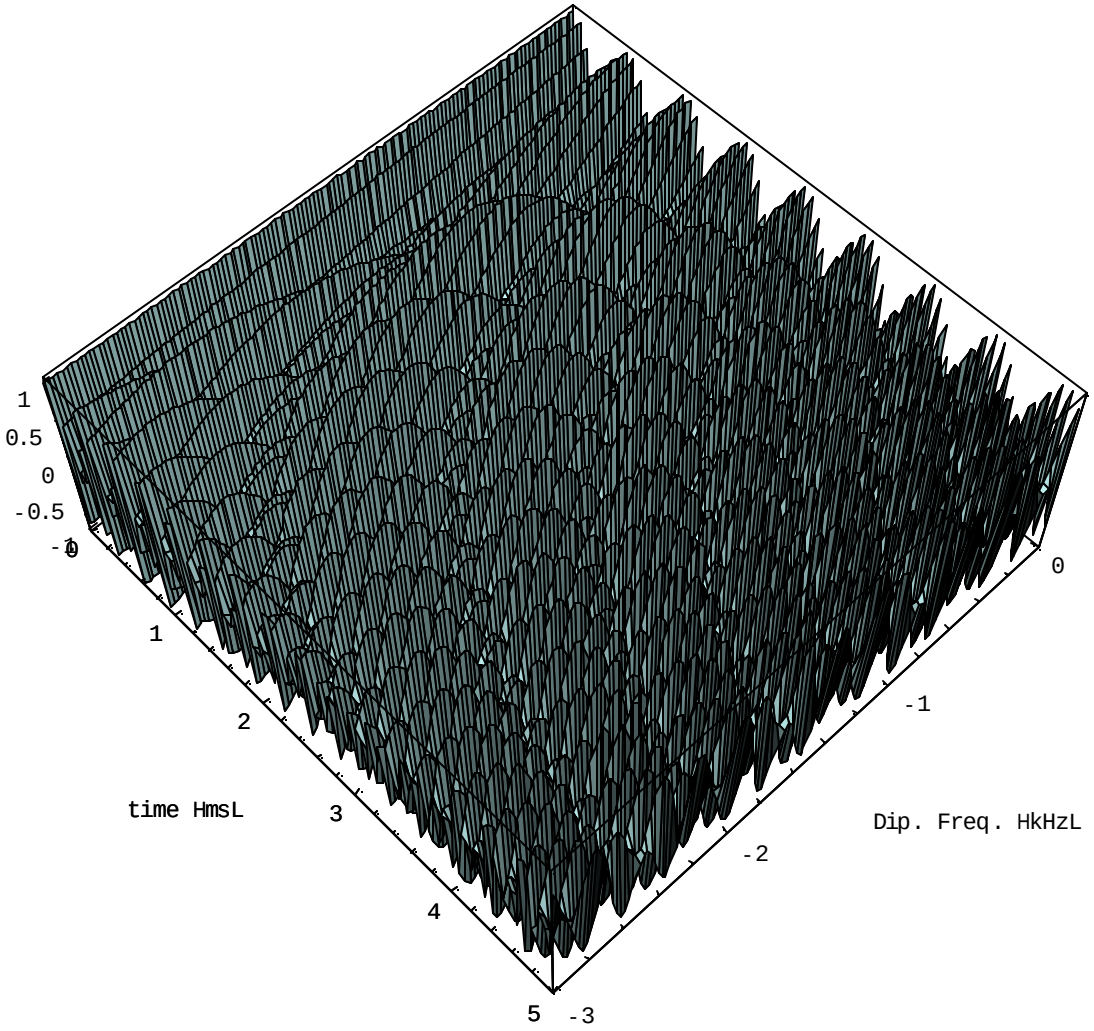

Figure 5-13: Graph of the CT function for the Ix self-magnetization for an oriented sample,, when $\sigma(0)=Ix$, as a function of the dipolar coupling frequency in the lab frame in kHz, and the chemical shift difference is set to Δ=120ppm and the CS average frequency (both in the lab frame) is set as Σ =80 ppm. The scalar coupling J=0. Time is in ms.

There are several characteristics in the CT from the transverse self-magnetization term that can be deduced from Eq. 5-23a. The first term, which we will call the "Ix even term" $\cos[0.5Bt]\cos[\Sigma t]\cos[0.5At]$ contains the B-term dipolar coefficient in a cosine as frequency 0.5B, modulated by a cosine dependent on the average of the chemical shift frequencies. It this term which retains the original dipolar coupling frequency in the cosine. The $\cos[\Sigma t]$ contribution from the chemical shift modifies the usual DCT form of the CT coefficients

The second term in Eq. 5-23a is equal to $\Delta/R \cos[0.5At] \sin[0.5Bt] \sin[\Sigma t]$. This will be called the "Ix odd" term as it is a function dependent on two sine terms which mix the chemical shift frequencies into a sine function of the dipolar coupling that is not present in the evolution of coherence from H_D (see Chapter 4, specifically Table 4-1a and b). The odd term in Ix has an amplitude modulated by the coefficient Δ/R which represents the contribution of the chemical shift difference Δ to the tilted frame. This amplitude acts to modulate the contribution of the second term in Eq. 5-23a, so that a small value of Δ results in only small contributions of the Ix odd term. The Ix coefficient is dominated by the Ix even term for small values of Δ, while the odd term will contribute significantly for larger values of Δ. Essentially, the Ix odd term results from the mixing of the chemical shift interaction into the coupling Hamiltonian.

Figure 5-3 graphs the dependence of Δ/R as a function of dipolar coupling and Δ, for when J=0 and J=53Hz. This represents the contribution of the second term in Eq. 5-23a over a range of dipolar coupling values important in ^{13}C homonuclear experiments on peptides. The range of Δ, representing the average of the chemical shifts in ppm, was chosen to illustrate the fast rise to full contribution; greater values of Δ follow an asymptotic rise towards the value of 1.

The even and odd transfer components of the Ix $\rightarrow$ Ix transfer coefficient are graphed in Figure 5-4a and 5-4b as a function of Δ and Σ to show the even and odd dependencies on both Σ and Δ. While Δ acts as the contribution of the Ix odd term to the

total coherence transfer, Σ acts as a superposing frequency over the DCT frequencies usually encountered during "pure" dipolar coupling.

The odd component in Ix also contains a sine term for the chemical shift contribution as well. As the difference in laboratory-frame chemical shifts (Δ) becomes smaller, that is, as the chemical shifts become equal, the sine term goes to zero as the term Δ/R → 0 and the total coherence transfer approaches

$$Ix \overset{H_T}{\rightarrow} Ix\cos[\frac{At}{2}]\cos[\frac{Bt}{2}]\cos[w_{cs}t]+o.t. \qquad (5\text{-}24a)$$

$$Ix \overset{H_T}{\rightarrow} Sx\sin[\frac{At}{2}]\sin[\frac{Bt}{2}]\cos[w_{cs}t]+o.t. \qquad (5\text{-}24b)$$

which are the expected dipolar coherence transfer terms multiplied by the average of the chemical shifts in the laboratory frame; since they are identical, it will be simply the shared chemical shift w_{cs} modulating the dipolar coherence transfer as a multiplicative frequency. This special case only occurs for nuclei sharing the same chemical shift.

Defining the dipolar coherence transfer frequency to represent two nuclei separated by 1.53 Å, the coherence transfer for the Ix "odd term" can be graphed as a function of both chemical shift frequencies in the laboratory frame in Figure 5-4. One can also vary the dipolar coupling and hold either Δ or Σ constant to examine the coupling for either the Ix odd term (Figures 5-5 and 5-6) and the Ix even term (Figure 5-7) as well as the Sx coefficient (Figures 5-8 through 5-10). It can be observed that each variable changes the value of the coherence transfer, making the value of the coherence transfer a five-variable function involving Δ, Σ, t, D, and J.

The behavior of the entire coherence transfer as a function of chemical shift values for the self magnetization Ix coefficient is a sum of the Ix odd and even terms, and is therefore heavily dependent on the value of the chemical shift difference. Figure 5-11 plots the complete form of the Ix → Ix coherence transfer for various values of the dipolar coupling against the chemical shift difference Δ, setting Σ constant at an arbitrary

50ppm, J at zero, and time at an arbitrary 1ms, which allows for easy viewing of the Δ-dependent trends in the self-magnetization. It is obvious that the value of Δ does modulate the contribution of the two terms to the CT. Additionally, Figure 5-12 shows the same plot for the variation in Σ, which acts as an additional modulation of the usual dipolar coherence transfer functions. Figure 5-13 gives the total coherence transfer as a function of time and dipolar coupling for arbitrary values of Δ and Σ. Compare this result to Figure 3-2a which has no chemical shift component. Even small values of the chemical shift can significantly change the behavior of the coherence transfer.

The transverse case of coherence transfer is much more complicated than the longitudinal case. The coherence transfer for the longitudinal case, Equation 5-25, for the Iz magnetization coefficient:

$$\sigma(0)=Iz \xrightarrow{H_t} \left(\frac{R^2 + ?^2 + B^2\cos[Bt]}{2R^2}\right)Iz + o.t. \qquad (5\text{-}25)$$

under the total Hamiltonian results in constant terms in R and Δ which predict that, as the chemical shift increases in comprison to the dipolar coupling frequency, longitudinal coherence transfer will disappear.

When one sets the chemical shift to zero, the Iz coefficient in Eq. 5-25 reduces to

$$\left(\frac{-B^2 + B^2\cos[Bt]}{2B^2}\right) = \frac{1}{2}(1+\cos[Bt]) \quad (5\text{-}26)$$

and returns the proper coefficient as seen for longitudinal coherence transfer under just H_D (see Table 4-1). Likewise, when the dipolar coherence transfer is zero, the coefficient reduces to 1, meaning there is no coherence transfer for σ(0)=Iz as expected. The chemical shift acts as an additional attenuating factor for Iz. Figure 5-5 shows the dependence of the coherence transfer of Iz on the chemical shift difference Δ in an oriented sample. Figure 5-14 and 5-15 graph the Iz and Sz coherence transfer respectively as a function of time and chemical shift difference Δ. Figures 5-16 and 5-17 correspond to a CT as a function of dipolar coupling and time for Iz and Sz when σ(0)=Iz.

The most apparent effect of appreciable chemical shift to the dipolar coupling in the longitudinal case is the dwindling of longitudinal coherence transfer between spins I and S. Looking, for example, at Figure 5-14, it is apparent that as Δ grows in magnitude, the system loses its ability to transfer coherence. This also predicts that nuclei with the same chemical shift, that is, when $\Delta=0$ will have the same coherence transfer behavior as a system with no chemical shift present, as there is no Σ-dependence within the longitudinal functions.

Examining Figures 5-16 and 5-17 for a single time constant of t=5ms, it is apparent that the CT is rapidly lost with an increase in Δ as compared to the dipolar coupling constant. Again, this shows that even over various dipolar coupling constants typical of ^{13}C experiments, CT is significantly reduced at t=5ms when Δ takes on the small value of 20ppm.

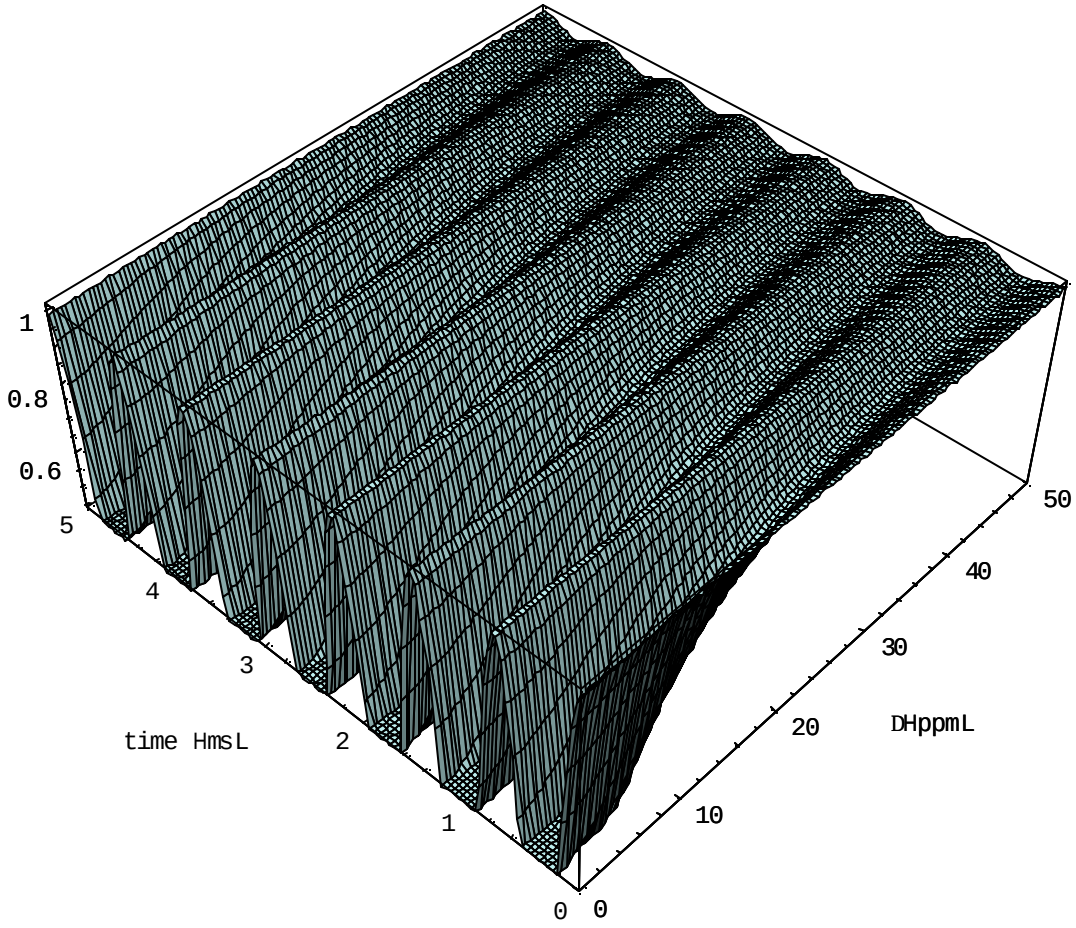

Figure 5-14: Graph of the CT function for the Iz self-magnetization for an oriented sample, when $\sigma(0)=Iz$, as a function of time and the chemical shift difference Δ in ppm. The dipolar coupling is set to correspond to an internuclear distance of 1.53 Å. The scalar coupling J=0. Time is in ms.

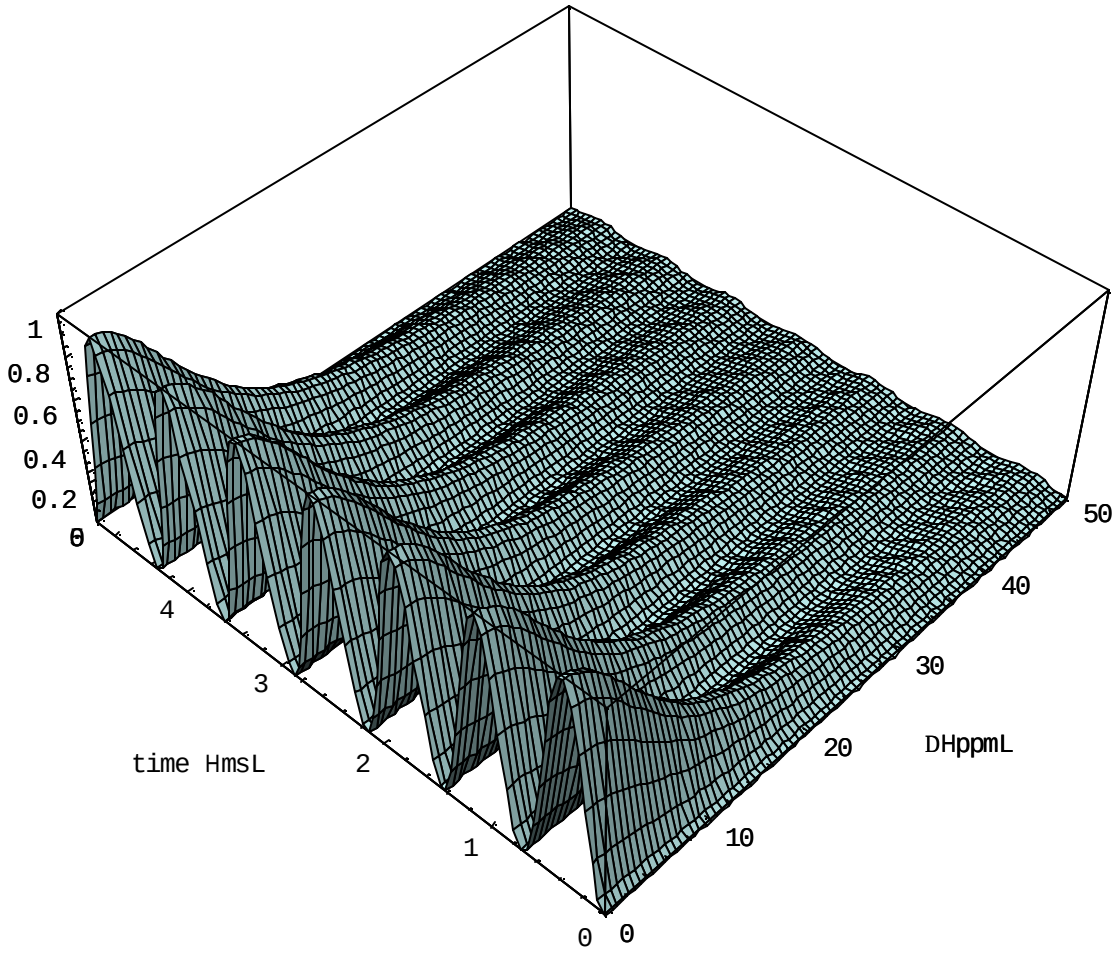

Figure 5-15: Graph of the CT function for the Sz transferred-magnetization for an oriented sample, when $\sigma(0)=Iz$, as a function of time and the chemical shift difference Δ in ppm. The dipolar coupling is set to correspond to an internuclear distance of 1.53 Å. The scalar coupling J=0. Time is in ms.

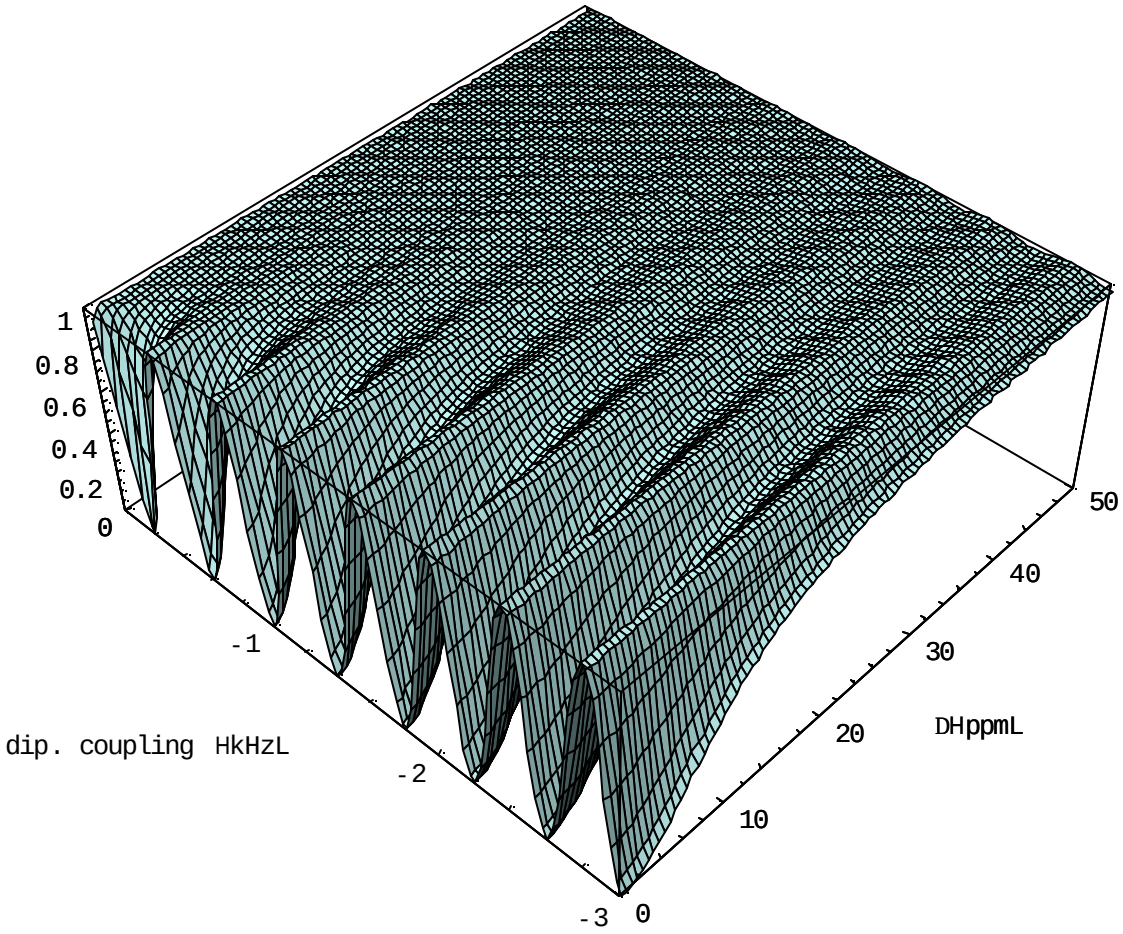

Figure 5-16: Graph of the CT function for the Iz self-magnetization for an oriented sample, when $\sigma(0)=Iz$, as a function of dipolar coupling frequency in kHz and the chemical shift difference Δ in ppm. The constant time is set to 5ms. The scalar coupling J=0.

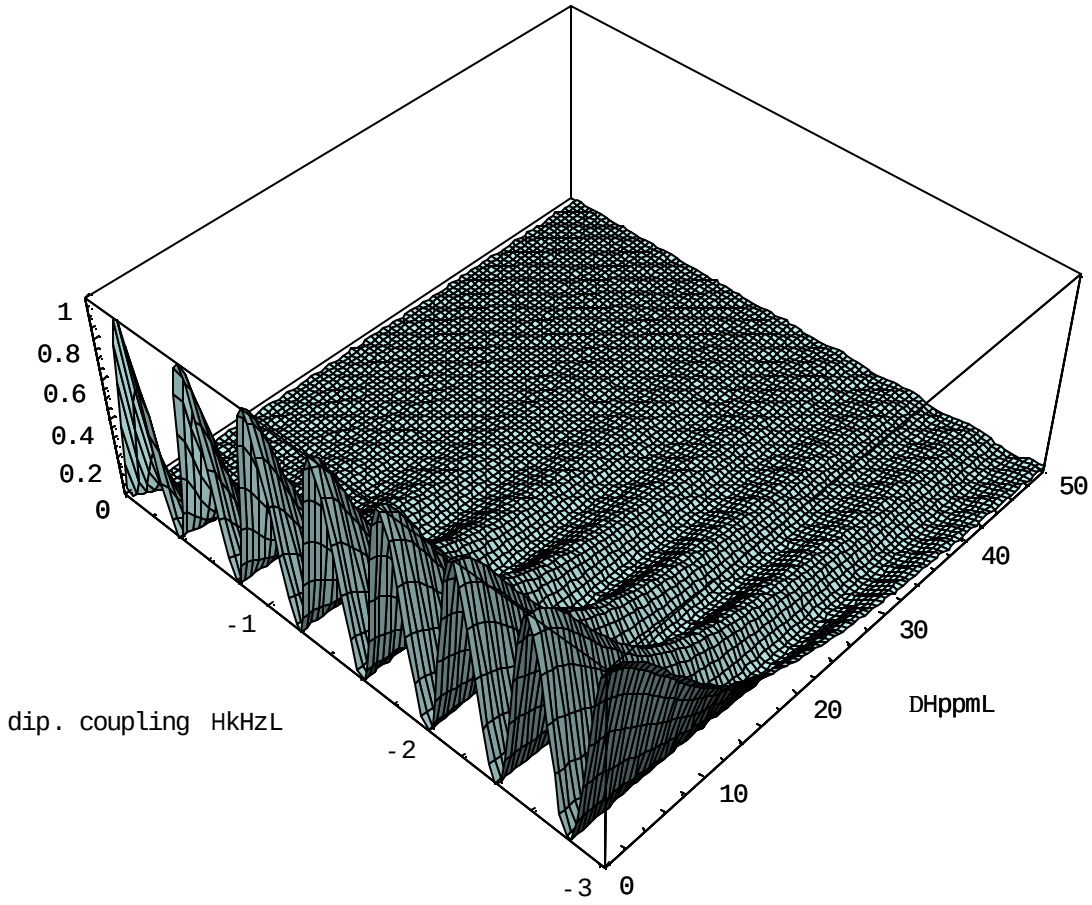

Figure 5-17: Graph of the CT function for the Sz transferred coherence for an oriented sample, when $\sigma(0)=Iz$, as a function of dipolar coupling frequency in kHz and the chemical shift difference Δ in ppm. The constant time is set to 5ms. The scalar coupling J=0.

The program IS.F was written (See Appendix A) which uses numerical calculations with the Wigner transformation matrices to transform the principal-axis system frequencies as in Equation 5-16 and then integrating over all possible angles in the longitudinal and transverse magnetization functions to simulate a powder averaging effect.

For longitudinal coherence transfer, simulations were done with parameters smaller in magnitude than or equal to those used for transverse magnetization modeling. Except for the very smallest anisotropies, the longitudinal equation was unable to transfer coherence; that is, the self-magnetization of spin I in state Iz remained constant over a sample time of up to 10ms. We therefore set out to model the transverse magnetization transfer exclusively.

The first step was to verify that the output of the program matched the case of pure DCT. Simulations were done with zero chemical shift as well as with equal chemical shifts. In the case of Iz -> Iz simulation, the sample returned the identical result to the pure dipolar recoupling case, as did the Ix simulation, both verified with comparison against the output of the POWDER.F program , also in the Appendix..

Simulations were performed with the FORTRAN program IS.F (see Appendix A) using inputs of: Euler angles from the spin 2 CS frame and for the spin 2 CS frame to the molecular frame, chemical shift principal values σ_{11}, σ_{22}, and σ_{33} for both spin 1 and spin 2, magic-angle sample spinning parameters, rotor tilt, dipolar coupling, and spin coupling. We chose an arbitrary C_α-C_O distance of 1.55 Å.

Figs. 5-18 through 5-23 all model the transverse coherence transfer in an unoriented sample for various parameters. Because the simulation is dependent on 22 separate parameters, an exhaustive examination of often-similar results would result in repetition. Instead, we look at various cases in each simulation run to see trends in the behaviors of the variables within the unoriented system simulations.

Varying the angles between the chemical shift PAS frame and the molecular frame had a noticeable effect on the rapid decay of coherence in the unoriented sample simulation. Adjusting the values of $\sigma_{11}=\sigma_{22}=\sigma_{33}$ for both spin I and spin S also made (expected) differences in the coherence transfer patterns. Figure 5-18 is a comparison between the conditions of no chemical shift (solid line), a small isotropic chemical shift in both nuclei (dashed line), and a small anisotropy of 5ppm in nucleus 1 (dashed-dot line). The left shoulder of the plot, falling from 100% magnetization (normalized to 1), can be followed for each of the examples as a measure for the rate of coherence transfer from spin I to spin S. The case of non-zero chemical shift yields a powder pattern familiar from Chapter 4 (Fig 4-1a) and is used as a comparison. The other two traces, those with nonzero chemical shift, show that the addition of chemical shift either aids in the loss of coherence due to a faster transverse dephasing, or actually increases the rate of coherent transfer to the second spin. To examine which case it might be, we model the response of the second spin, Sx, whose coefficient (from Eq. 5-21) is

$$\frac{B}{R}\cos(\Sigma t)\sin(\tfrac{At}{2})\sin(\tfrac{Bt}{2}) \qquad (5\text{-}27)$$

Figure 5-19 models the case of the Sx magnetization when the initial state $\sigma(0) = Ix$. Although it is understood that introduction of a chemical shift interaction reduces the transfer of transverse coherent magnetization, it was pleasant to see that the analytical solution yielded the same results. It can be seen that even for a small chemical shift (10 ppm) in the two nuclei, the addition of chemical shift has decreased both the magnitude of the resulting transverse magnetization and the speed at which it is transferred, as the shoulder obviously lags behind that for the pure coupling Hamiltonian (solid line). Adding a small anisotropy (3 ppm) to the sample does change the phase pattern of the curve, but does not appreciably impact the coherence transfer rate. Examining Eq. 5-27 once again, it can be seen that the greater the difference in the chemical shifts of the two nuclei, at each angle in the crystallite sampling, the smaller the

term B/R will become, reducing the coherence transfer magnitude for Sx, eventually by the reciprocal of the chemical shift difference Δ. For Sx, the term cos(Σt), sampled for each crystallite orientation, will also begin to dominate the powder pattern for greater values of Σ, resulting in a wider range of frequencies and therefore a faster decay of transverse magnetization. In comparison, as Δ increases, the Ix self-magnetization gains the full contribution of the "odd term." If the difference in chemical shift decreases transverse coherent transfer of magnetization, then where does the coherence go?

Comparing Eq. 5-21 to the results of Chapter 3 shows that new coherences arise as compared to the simple case of DCT free of chemical shift. The operators that appear that seem "out of the ordinary" are Iy, Sy, IxSz, all of which operators are outside the coherent transfer group discussed in Chapter 2. In fact, the cylindrical symmetry of DCT is broken by any anisotropy in the chemical shift, which manifests as the term Δ. This symmetry breaking reduces the coherent transfer of magentization since the transfer is no longer contained in the cyclical groups shown in Table 2-1. Therefore, the effect of anisotropies in the chemical shift act to break the symmetry of cylindrical mixing present in the dipolar Hamiltonian.

The chemical shift is a transverse interaction which breaks the cylindrical symmetry apparent in the spin operators of H_D. As the chemical shift difference increases to a magnitude much larger than the dipolar coupling term B (Eq. 5-19f), the coherence becomes shared equally among the antiphase operators (-IySz, IxSz) and the transverse operators (Iy, Ix). The fact that these operators dominate, and longitudinal CT is impossible, means that the effects of chemical shift act as a kind of dissapative rip in the symmetry present in the dipolar Hamiltonian. Zero- and double-quantum operators cannot be generated during free evolution in the presence of chemical shift, unlike in the case of dipolar coupling where the Iz group of Table 2-5 has IxSy and IySx as members. Therefore, magnetization cannot be "stored" in unobservable operators when DCT operates in the presence of chemical shift.

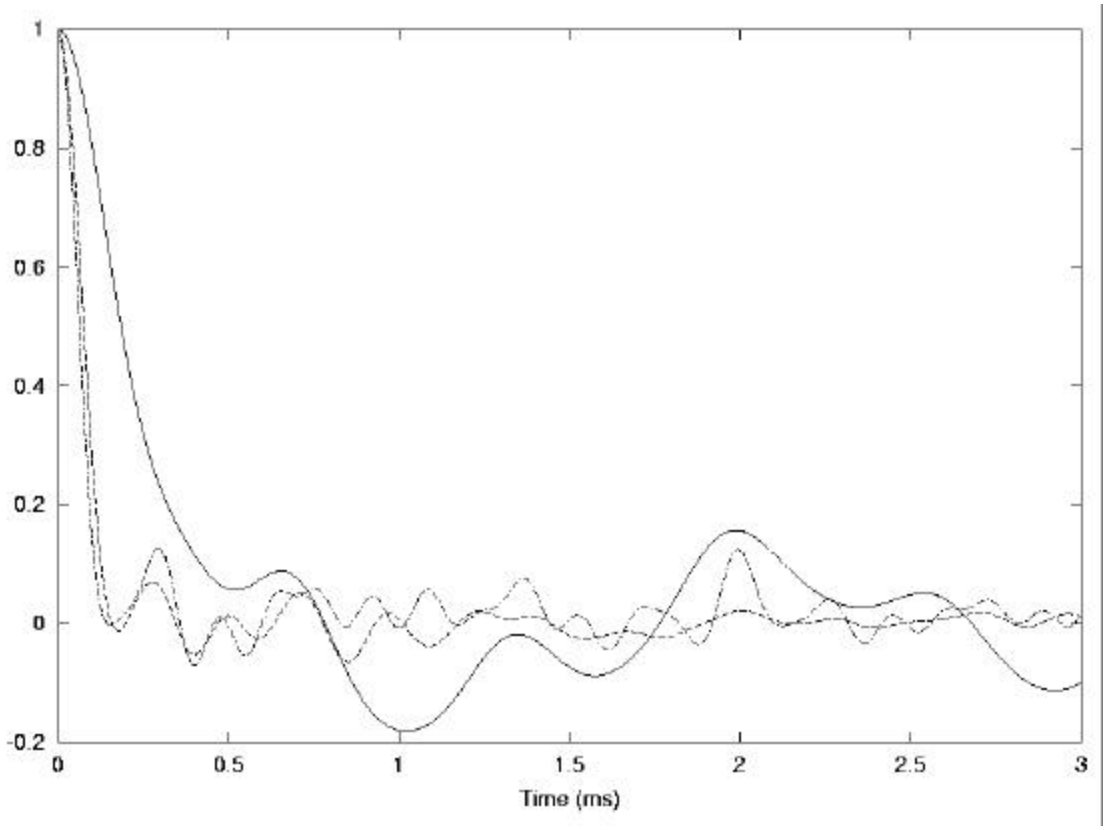

Figure 5-18: Graph of the CT function for the Ix self-magnetization of an unoriented sample, when σ(0)=Ix, as a function of time. The parameters are given below. All three simulations share the listed constants, with specific principal values given below: The Euler angles were chosen arbitrarily. Note that the "chaotic" behavior of the dephasing is not due to the limits of resolution.

Shared:
600., 6727., 1.55, 0. H larmor magnet, gamma, internuc dist in angs, J in Hz
400, 3.0, 200 Steps in angle summation, sim. time (ms), graph points
10., 75., 50. Euler angles from cs PAS to dipolar frame for spin I
20., 145.,90 Euler angles from cs PAS to dipolar frame for spin S
0.0001,54.7,0.0 Zero, rotor-B0 angle, wr*t both in degrees from rotor to lab

Solid line:
0.,0.,0. σ11, σ22, σ33 for spin I (ppm)
0.,0.,0 σ11, σ22, σ33 for spin S (ppm)

Dashed line:
15.,10.,10. σ11, σ22, σ33 for spin I (ppm)
10.,10.,10 σ11, σ22, σ33 for spin S (ppm)

Dashed-dot line:
10.,10.,10. σ11, σ22, σ33 for spin I (ppm)
10.,10.,10 σ11, σ22, σ33 for spin S (ppm)

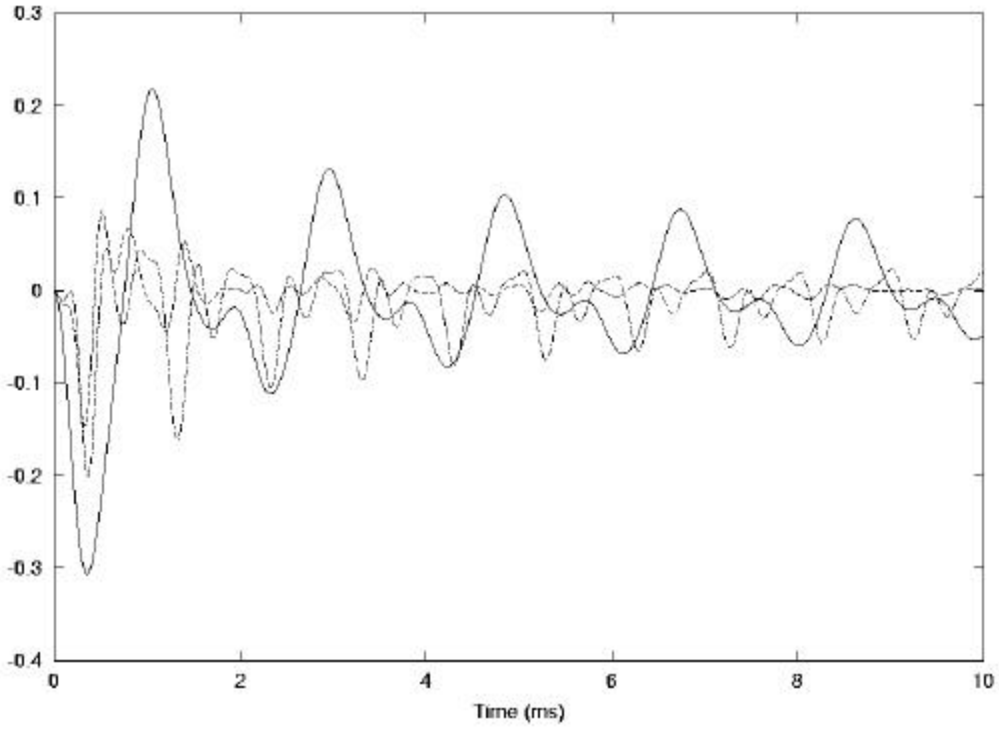

Figure 5-19: Graph of the CT function for the Sx (transferred) self-magnetization for an unoriented sample, when σ(0)=Ix, as a function of time. The parameters are given below. Note that the "chaotic" behavior of the dephasing is not due to the limits of resolution. Euler angles were chosen arbitrarily. Note that the "chaotic" behavior of the dephasing is not due to the limits of resolution.

Both simulations use the following parameters, with the differences given below.

600., 6727., 1.55, 0. H larmor magnet, gamma, internuc dist in angs, J in Hz
500, 10.0, 500 Steps in angle summation, sim. time (ms), graph points.
10., 75., 50. Euler angles from cs PAS to dipolar frame for spin I
20., 145.,90 Euler angles from cs PAS to dipolar frame for spin S
0.0, 54.7, 0.0 Zero, rotor to B0 angle, wr*t both in degrees from rotor to lab

Solid line:
0.,0.,0. σ11, σ 22, σ33 for spin I
0.,0.,0. ……σ11, σ22, σ33 for spin S

Dashed line:
13.,10.,10. σ11, σ 22, σ33 for spin I
13.,10.,10. ……σ11, σ22, σ33 for spin S

Dashed-dot line:
10.,10.,10. σ11, σ 22, σ33 for spin I
10.,10.,10. ……σ11, σ22, σ33 for spin S

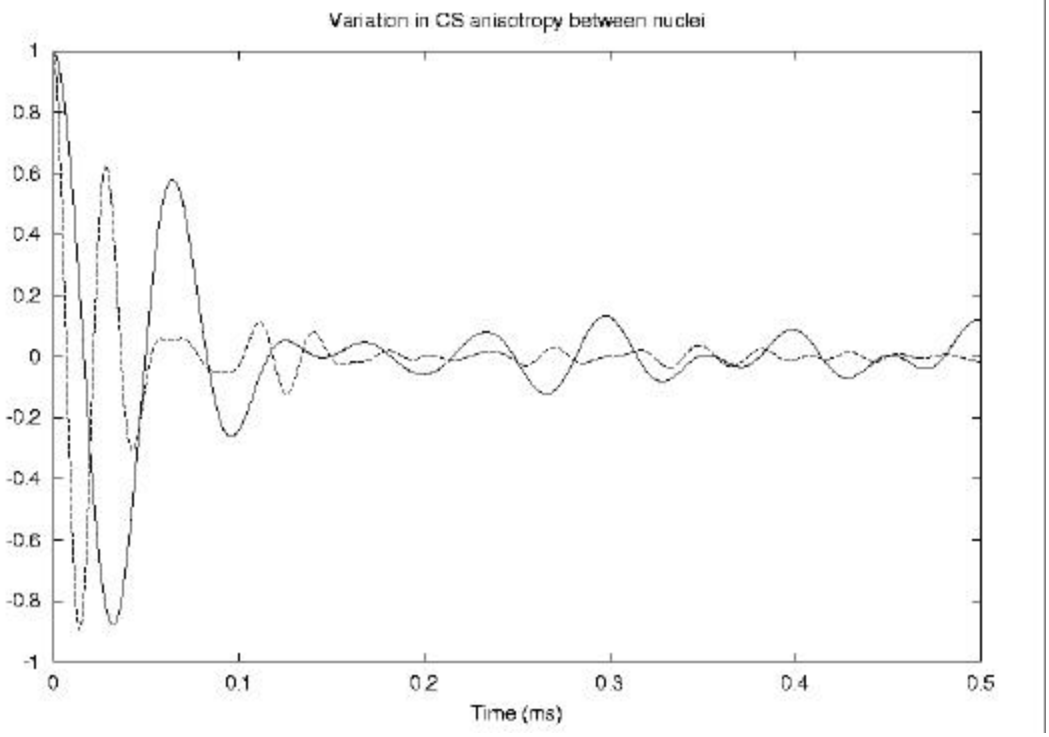

Figure 5-20: Graph of the CT function for the Ix self-magnetization for an unoriented sample, when σ(0)=Ix, as a function of time for two sets of principle values of the chemical shift. The parameters are given below. Note that the "chaotic" behavior of the dephasing is not due to the limits of resolution.

All lines have the following values in common:
600., 6727., 1.55, 0. H larmor magnet, gamma, internuc dist in angs, J in Hz.
400, 0.05,200 Steps in angle summation, sim. time (ms), time steps.
90. 172. 15. Euler angles from cs PAS to dipolar frame for spin I
40. 30. 164. Euler angles from cs PAS to dipolar frame for spin S
0., 0., 0. Zero, rotor to B0 angle, wr*t both in degrees from rotor to lab

Solid line:
100.,100.,100. σ11, σ22, σ33 for spin I (ppm)
100.,100.,100 σ11, σ22, σ33 for spin S (ppm)

Dashed line:
300. 100. 300. σ11, σ22, σ33 for spin I (ppm)
300. 300. 100 σ11, σ22, σ33 for spin S (ppm)

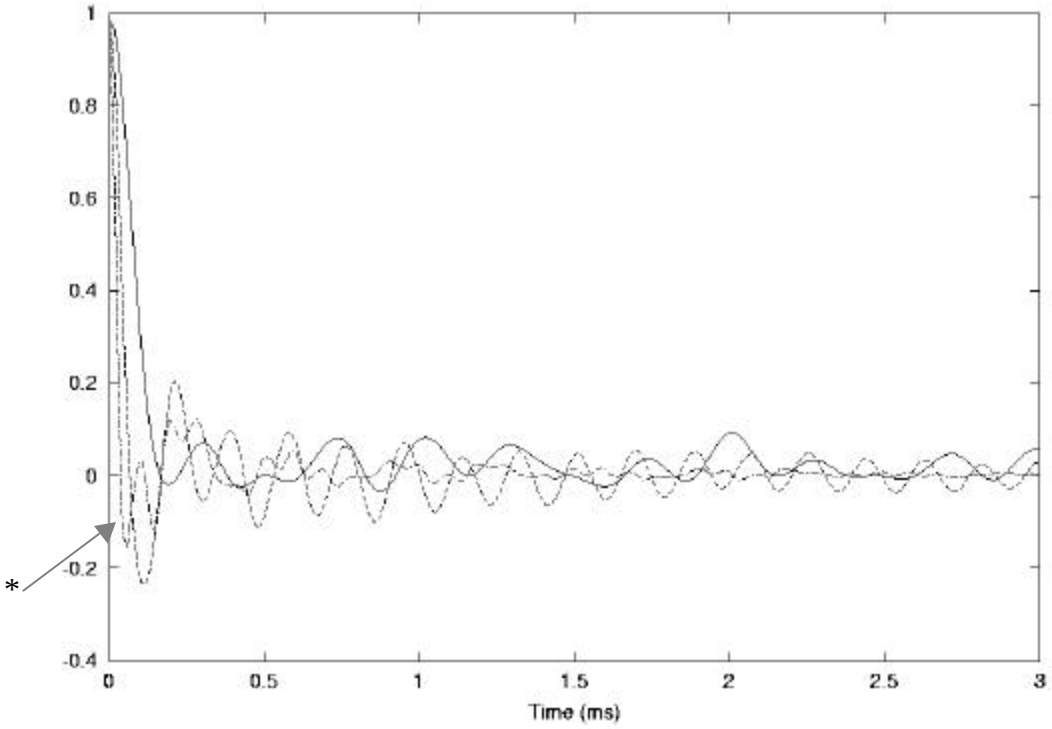

Figure 5-21: Graph of the CT function for the Ix self-magnetization for an unoriented sample, when σ(0)=Ix, as a function of time for three sets of principal values of the chemical shift. The parameters are given below. Note that the "chaotic" behavior of the dephasing is not due to the limits of resolution.

All lines have the following values in common:
600., 6727., 1.55, 0. H larmor magnet, gamma, internuc dist in angs, J in Hz.
400, 0.05,200 Steps in angle summation, sim. time (ms), time steps.
90. 172. 15. Euler angles from cs PAS to dipolar frame for spin I
40. 30. 164. Euler angles from cs PAS to dipolar frame for spin S
0., 0., 0. Zero, rotor to B0 angle, wr*t both in degrees from rotor to lab

Solid line:
10.,10.,10. σ11, σ22, σ33 for spin I (ppm)
10.,10.,10 σ11, σ22, σ33 for spin S (ppm)

Dashed line:
10.,10.,50. σ11, σ22, σ33 for spin I (ppm)
10.,10.,50 σ11, σ22, σ33 for spin S (ppm)

Dashed -dot line (marked with * and the fastest decay)
10. 10. 100. σ11, σ22, σ33 for spin I (ppm)
10. 10. 100 σ11, σ22, σ33 for spin S (ppm)

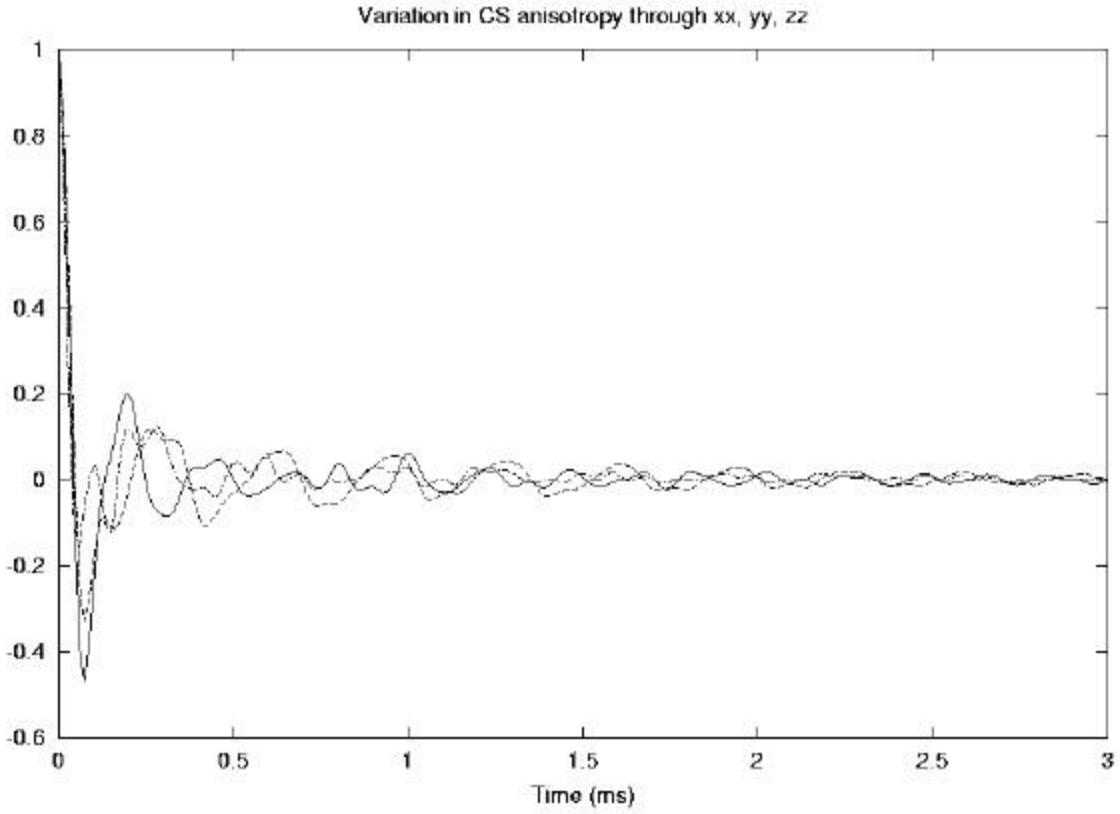

Figure 5-22: Graph of the CT function for the Ix self-magnetization for an unoriented sample, when σ(0)=Ix, as a function of time for three sets of principal values of the chemical shift. The parameters are given below. Note that the "chaotic" behavior of the dephasing is not due to the limits of resolution.

All lines have the following values in common:
600., 6727., 1.55, 0. H larmor magnet, gamma, internuc dist in angs, J in Hz.
400, 0.05,200 Steps in angle summation, sim. time (ms), time steps.
90. 172. 15. Euler angles from cs PAS to dipolar frame for spin I
40. 30. 164. Euler angles from cs PAS to dipolar frame for spin S
0., 0., 0. Zero, rotor to B0 angle, wr*t both in degrees from rotor to lab

Solid line:
100,10.,10. σ11, σ22, σ33 for spin I (ppm)
100.,10.,10 σ11, σ22, σ33 for spin S (ppm)

Dashed line:
10.,100.,10. σ11, σ22, σ33 for spin I (ppm)
10.,100.,10 σ11, σ22, σ33 for spin S (ppm)

Dashed -dot line
10. 10. 100. σ11, σ22, σ33 for spin I (ppm)
10. 10. 100 σ11, σ22, σ33 for spin S (ppm)

The anisotropy of chemical shift seems to affect the rapidity of dephasing. Figure 5-20 is an example of extreme variations in the anisotropy between two nuclei. It can be easily seen that while the pattern of evolution is affected, the added anisotropy causes a rapid loss of coherence in the Ix self-magnetization.

Figure 5-21 gives an example of the change in coherence transfer when only one set of anisotropies (along σ_{zz}) is varied. The coherence loss in Ix becomes more rapid for greater values of σ_{zz}.

Fig 5-22 shows that the variation of the most anisotropic CS principal value does not change the rate of coherence loss in Ix, which can be seen by the decay of the shoulder to the left of the graph. This leads to the conclusion that the same isotropic chemical shift with the same angles between the chemical shift PAS and the dipolar PAS will yield the same coherence transfer rate, no matter what the individual principal axis values might be.

Conclusions

This work has given the simple analytical results for the coherence transfer in the presence of chemical shift. Examination of the analytical equations sheds light on the reasons for many well-known experimental facts.

Dipolar coherence transfer in the presence of chemical shift is much reduced. Even in oriented samples, the rapid dephasing due to (even small) anisotropic chemical shifts can cause coherence transfer to be rapidly lost as we have seen in the simulations earlier in this chapter. The dephasing in unoriented samples with small chemical shifts is of sufficient rapidity to cause the dipolar coherence transfer to be rapidly lost to dephasing processes. The solution, as always, involves experimentally maniplulating the chemical shift. This is especially true when attempting to transfer longitudinal

magnetization, which loses coherence transfer ability for even small values of the chemical shift.